Hindawi Publishing Corporation
Advances in Tribology
Volume 2015, Article ID 182713, 7 pages
http://dx.doi.org/10.1155/2015/182713

Research Article

Effect of L/D Ratio on the Performance of Two-Lobe Pressure Dam Bearing: Micropolar Lubricated

Sanyam Sharma and C. M. Krishna

Maulana Azad National Institute of Technology, Bhopal 462051, India

Correspondence should be addressed to Sanyam Sharma; sanyammee@rediffmail.com

Received 16 December 2014; Revised 3 February 2015; Accepted 5 February 2015

Academic Editor: Michel Fillon

Two-lobe pressure dam bearings are commonly used in high speed rotating machineries. Their use is considered more stable than plain cylindrical bearings. Such bearings have a dam in the upper half whereas the lower half is provided with a relief track. Performance of two-lobe pressure dam bearings under micropolar fluid is evaluated. Finite element method is used to solve the modified Reynolds equation. Fluid film pressures are obtained by solving modified Reynolds equation. Thus pressure obtained is used to find performance characteristics of this bearing. The dynamic performance characteristics are studied at various L/D ratios. Three L/D ratios are considered 1.6, 2.0, and 2.4 for the analysis purpose. Results obtained are presented for various micropolar parameters. Results show that stability of two-lobe pressure dam bearings increases with decrease in aspect ratio (L/D).

1. Introduction

Pressure dam bearing is widely acceptable in high speed rotating machineries due to its good stability characteristics over plain two-lobe bearing. Lobed bearing came into existence, to overcome the limitations of circular bearing such as low load carrying capacity, stiffness, and stability. Effect of L/D ratios on the stability of circular bearing was discussed by [1–3]. They found that L/D ratio affects the stability up to some extent. Therefore, researchers showed interest to examine the noncircular (lobed) bearing. The analysis of lobed bearing was given by [4–7]. These researchers analyzed the performances of such bearings and found that lobed bearings were much better in stability, which was the main problem of high speed rotating machineries. The problem was minimized by changing the bearing geometry from circular to lobed but could not be eliminated completely. Further, researchers continued work on the stability criterion and investigated circular and noncircular bearings by cutting a step (pressure dam) and relief rack in bottom half. Circular bearing with pressure dam was examined by [8, 9] and different variants of lobed bearing providing pressure dam were analyzed such as two-lobe by [10, 11] and three-lobe by [12, 13]. All the researchers engaged in analysis of lobed bearing with pressure dam concluded that the performance of pressure dam bearing was better than plain lobed bearing (without pressure dam).

Due to the contamination of dirt or foreign particles in the commercial lubricant, classical fluid theory does not work well. Therefore to solve the lubrication problem [14] develops micropolar fluid theory. Micropolar fluids are fluids with microstructure. They contain rigid, randomly oriented, or spherical particles suspended in viscous medium. To increase effectiveness of the Newtonian lubricants, polymer additives are mixed to the Newtonian lubricant in order to improve their performance characteristics and then such fluid behaves as micropolar fluid. Increase in the viscosity of such lubricant is also observed as the additives are introduced in Newtonian lubricant. Load carrying capacity increases as the concentration of additives and contaminants increases [15]. There are many physical examples of micropolar fluids as ferrofluids, blood flows, bubbly liquids, and liquid crystals [16] in nuclear power plant where heat transfer agent sodium is used as a micropolar lubricant [17].

As per the Eringens [14] theory, micropolar fluid was superior in comparison to Newtonian fluid. Higher threshold of stability was achieved [18] in circular bearing with micropolar lubrication. Lobed bearings were examined

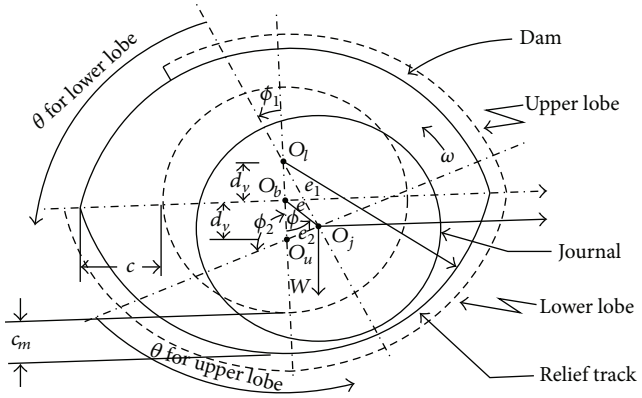

FIGURE 1: Two-lobe pressure dam bearing.

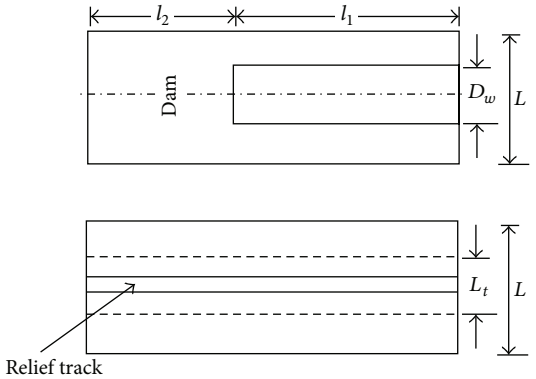

FIGURE 2: Pressure dam geometry.

by [19, 20]. Rahmatabadi et al. [19] extended the work of Das et al. [18] for the analysis of lobed bearing under micropolar lubrication and investigated the static performance of lobed bearing and observed that micropolar lubricants could produce significant increase in the static performance characteristics. Rahmatabadi et al. [20] considered the effects of bearing orientation on the performance of lobed bearing and reported that the performance of the two-lobe bearing was significantly affected by the bearing orientation, as the number of lobes in a bearing was increased.

During the literature survey, author found that few researchers [21] worked on two-lobe bearing with pressure dam. Since micropolar fluid is found to have considerable effect on the performance characteristics of two-lobe pressure dam bearing, it is expected that the performance of two-lobe pressure dam bearing system will also be affected. This present paper deals with the effect of L/D ratio on the dynamic performance of two-lobe pressure dam bearing.

2. Bearing Geometry

Performance analysis of such bearing is obtained by adding the individual lobe performance evaluated separately. The upper lobe is provided with pressure dam and lower lobe with

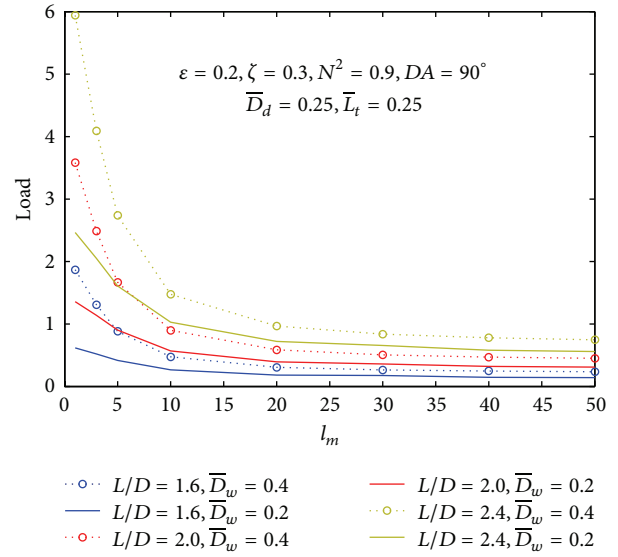

FIGURE 3: Load variation as a function of characteristics length "l_m."

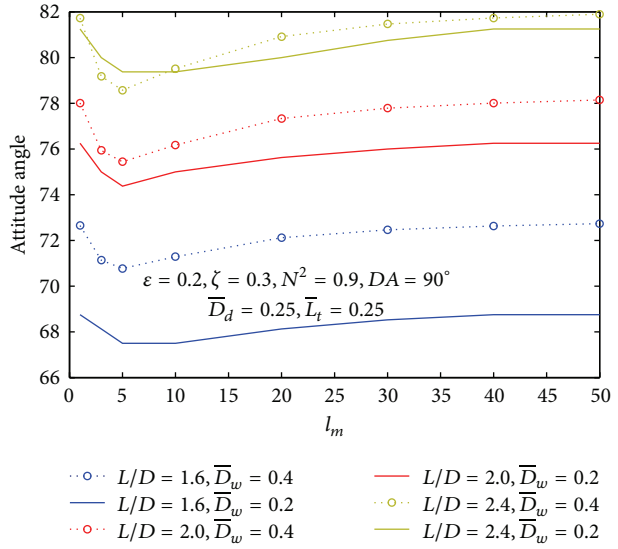

FIGURE 4: Attitude angle variation as a function of characteristics length "l_m."

relief track is shown in Figures 1 and 2. Lengths l_1 and l_2 are circumferential lengths before and after dam. Consider

$$\varepsilon_1^2 = \varepsilon^2 + \delta_v^2 + 2\varepsilon\delta_v \cos\phi,$$

$$\varepsilon_2^2 = \varepsilon^2 + \delta_v^2 - 2\varepsilon\delta_v \cos\phi,$$

$$\phi_1 = \tan^{-1}\left[\frac{\varepsilon \sin\phi}{\varepsilon\cos\phi + \delta_v}\right]\frac{180}{\pi}, \quad (1)$$

$$\phi_2 = \tan^{-1}\left[\frac{\varepsilon \sin\phi}{\varepsilon\cos\phi - \delta_v}\right]\frac{180}{\pi}.$$

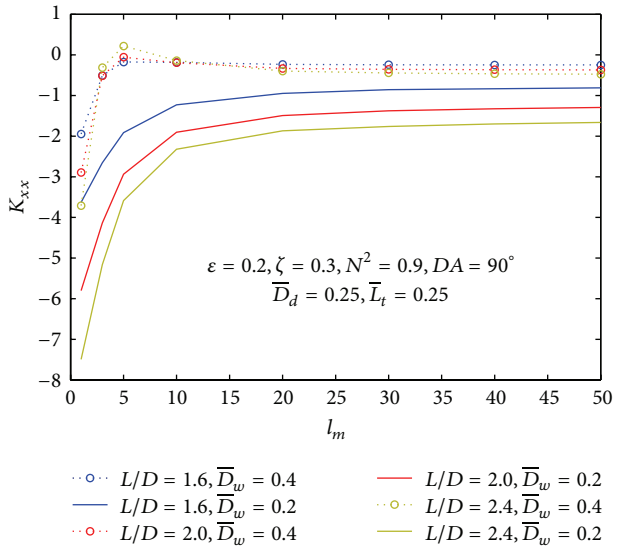

Figure 5: Variation of K_{xx} as a function of characteristics length "l_m."

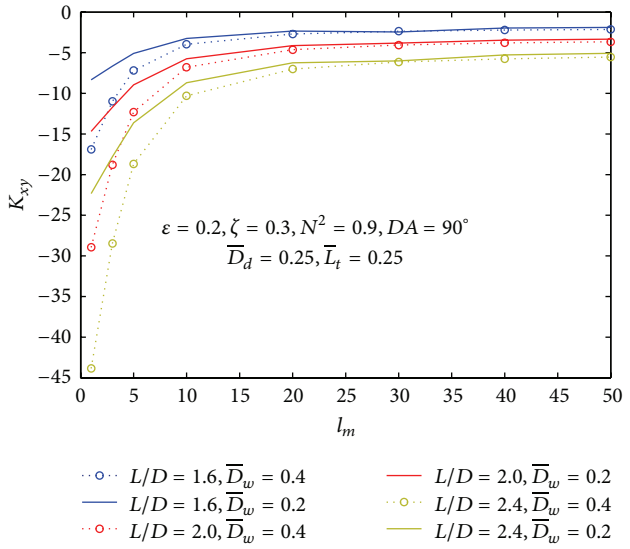

Figure 6: Variation of K_{xy} as a function of characteristics length "l_m."

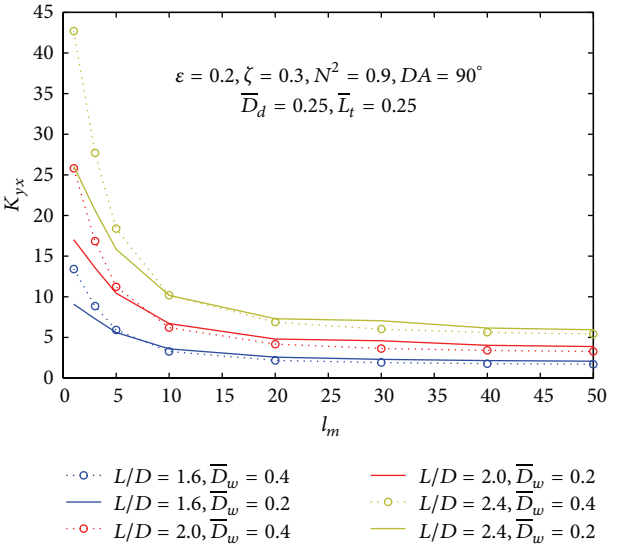

Figure 7: Variation of K_{yx} as a function of characteristics length "l_m."

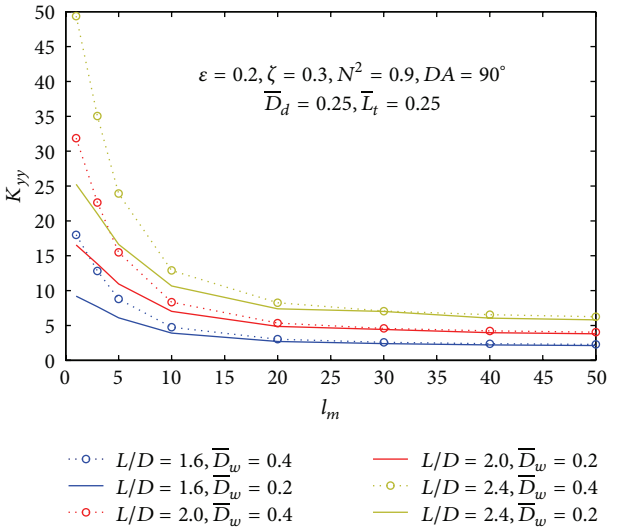

Figure 8: Variation of K_{yy} as a function of characteristics length "l_m."

3. Analysis

3.1. Modified Reynolds Equation. Based on [18] work the generalized form of the Reynolds equation for micropolar fluids is given below:

$$\frac{\partial}{\partial\theta}\left[\frac{\psi\left(\Lambda, N, \overline{h}\right)}{\mu}\frac{\partial\overline{p}}{\partial\theta}\right] + \left(\frac{R}{L}\right)\cdot\frac{^2\partial}{\partial z}\left[\frac{\psi\left(\Lambda, N, \overline{h}\right)}{\mu}\frac{\partial\overline{p}}{\partial z}\right] = \frac{\partial\overline{h}}{\partial\theta} + 12\frac{\partial\overline{h}}{\partial t}, \quad (2)$$

where

$$\phi\left(\Lambda, N, \overline{h}\right) = \overline{h}^3 + 12\frac{\overline{h}}{l_m^{\,2}} - 6\frac{N\overline{h}^2}{l_m}\coth\left(\frac{N\overline{h}l_m}{2}\right). \quad (3)$$

N^2 and Λ are the two important parameters of a micropolar fluid. Linear and angular momentum equations are coupled by a parameter N^2, called the coupling number; the second nondimensional parameter is the characteristic length (l_m) which represents the interaction between the bearing geometry and fluid film. l_m depend on the size of the lubricant molecules. At smaller l_m the effect of microstructure is very pronounced. Lower values of l_m mean the larger values of the characteristic length ($l_m = C/\Lambda$). Thus, small

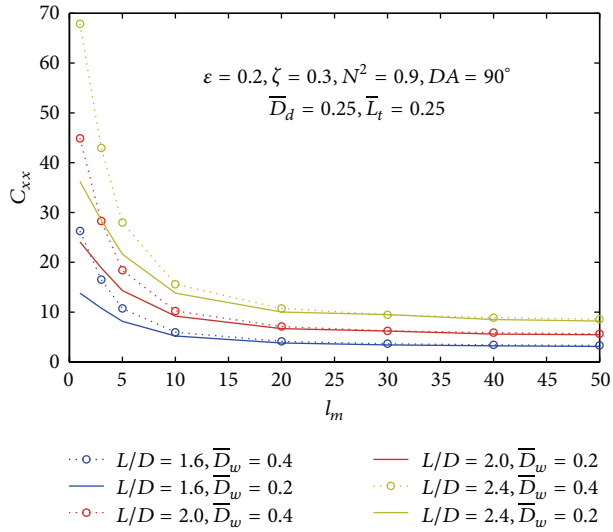

FIGURE 9: Variation of C_{xx} as a function of characteristics length "l_m."

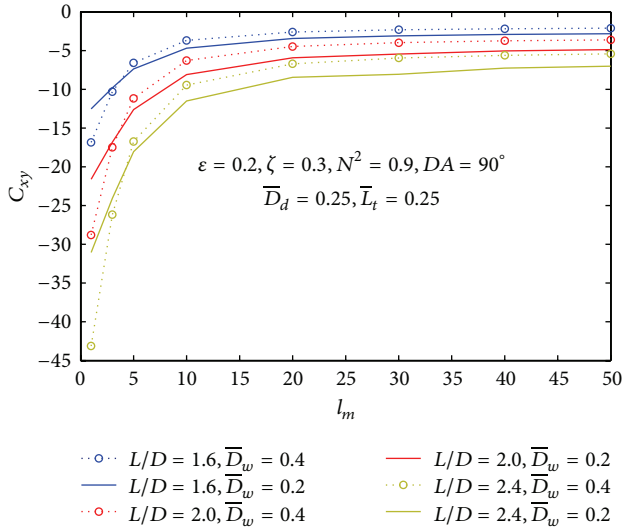

FIGURE 10: Variation of C_{xy} as a function of characteristics length "l_m."

l_m indicates that characteristic length of the substructure is larger compared to that of clearance dimension. At high l_m values, the effect of substructure becomes less significant and in the limiting case when $l_m \to \infty$, the effect of individuality of the substructure is lost and the lubricant reduces to Newtonian one. The following dimensionless quantities are used:

$$l_m = \frac{c}{\Lambda}, \qquad \theta = \frac{x}{R}, \qquad \overline{Z} = \frac{Z}{L},$$
$$\overline{h} = \frac{h}{c_m}, \qquad \overline{p} = \frac{p{c_m}^2}{\mu U R}. \tag{4}$$

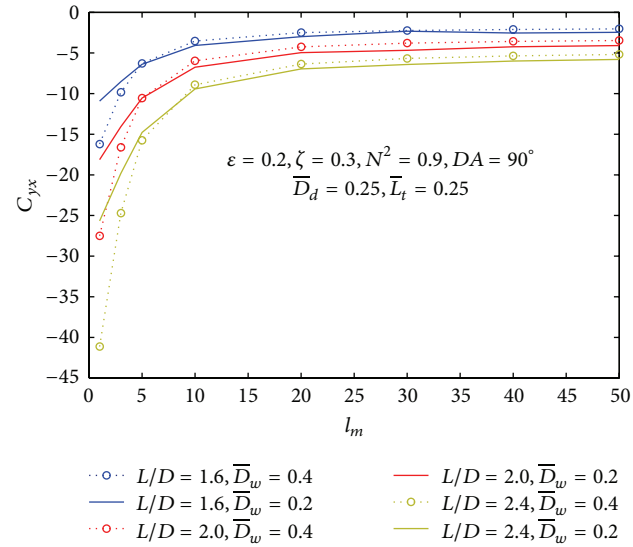

FIGURE 11: Variation of C_{yx} as a function of characteristics length "l_m."

Pressure boundary conditions are applied:

$$\overline{P}\left(\theta, \overline{Z}\right) = 0 \quad \text{at } \theta = 0, \theta_2$$
$$\overline{P}\left(\theta, \overline{Z}\right) = 0 \quad \text{at } \overline{z} = \pm 1 \tag{5}$$
$$\frac{\partial \overline{p}}{\partial \theta}(\theta, z) = 0 \quad \text{at } \theta = \theta_2.$$

3.2. Solution Procedure. Equation (2) is solved by finite element method, using Galerkin's approach. The domain is divided into four noded isoparametric elements, such as 100 elements in circumferential direction and 120 elements in the axial direction. The elements matrices are generated for all elements and assembled to get global coefficient matrix. Thus finite element equations are obtained. Fluid film pressures are computed at nodal points by applying Reynolds' boundary conditions as given in (5).

4. Results and Discussion

Various dynamic characteristics are presented in the form of plots for three different L/D ratios as shown in Table 1 while other parameters are held constant like eccentricity ratio (ε), ellipticity ratio (ζ), coupling number (N^2), dam depth, and relief track length. The values of characteristics length l_m are chosen (1–50), as beyond the $l_m = 50$, all the performance characteristics were found to be independent of "l_m" beyond the value $l_m = 50$. This is the typical range taken by all researchers.

Figure 3 depicts that load carrying capacity increases as there is increase in L/D ratio and is found to be maximum at aspect ratio 2.4. It means at higher L/D ratio the bearing can sustain higher load. For a particular value of L/D ratio, it is observed that load is higher at lower value of characteristics

Table 1: Parameters for two-lobe pressure dam bearing.

Bearing geometry parameters	
Aspect ratio L/D	1.6, 2.0, 2.4
Operating parameters	
Eccentricity ratio ε	0.20
Ellipticity ratio ζ	0.3
Dam parameters	
Dam width ratio $\overline{D}_w$	0.4, 0.2
Dam depth ratio $\overline{D}_d$	0.25
Relief track width ratio $\overline{L}_t$	0.25
Micropolar parameters	
Coupling number N^2	0.9
Characteristics length l_m	1, 3, 5, 10, 20, 40, 50

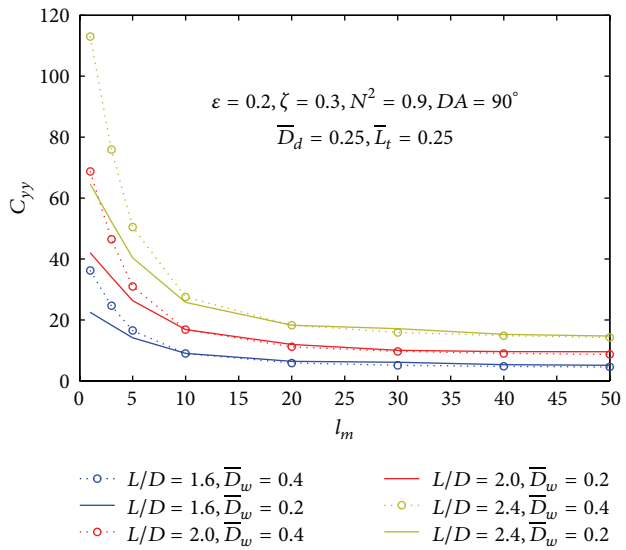

Figure 12: Variation of C_{yy} as a function of characteristics length "l_m."

length (l_m) and decreases as l_m increases. Load capacity is higher at higher value of D_w. Figure 4 shows that attitude angle increases as there is increase in L/D ratio and it is found to be maximum at aspect ratio 2.4. It means at higher L/D ratio of the bearing, for a particular value of L/D ratio, it is observed that attitude angle is higher at lower value of characteristics length (l_m) and decreases as characteristics length (l_m) decreases. It is also observed that there is a minimum attitude angle for each L/D ratio. Attitude angle is observed higher at larger dam width ratio. Figure 5 depicts that K_{xx} first increases for lower values of l_m and then becomes constant for the higher values of characteristics lengths. Higher material length does not produce much effect on the stiffness K_{xx}. Figure 6 depicts that K_{xy} is found to be maximum at smaller L/D ratio 1.6. It is observed that K_{xy} is higher at lower value of characteristics length (l_m) and decreases as l_m decreases. Figures 7, 8, and 9 show the behavior

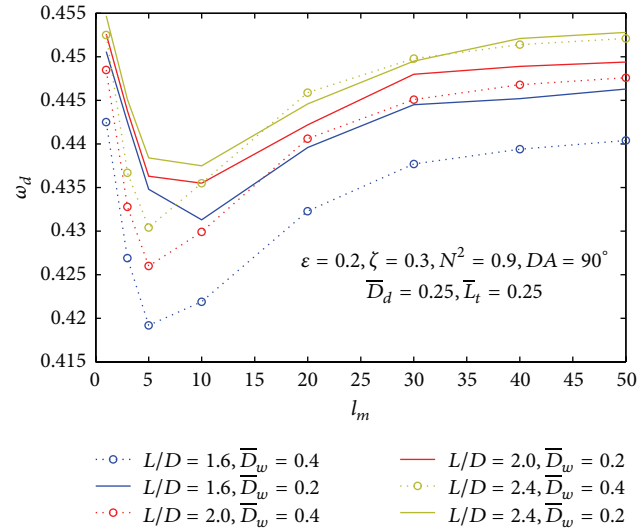

Figure 13: Variation of damped frequency of whirl ω_d as a function of characteristics length "l_m."

of K_{yy}, C_{xx}, and C_{xy}, respectively, and show that all the three are on the same trend. These stiffness coefficients are found on higher side, as L/D ratio increases. For all values of L/D ratio these coefficients decrease as l_m increases. Figures 10 and 11 show the behavior of cross coupling stiffness C_{xy} and C_{yx}, respectively, and depict that these coefficients decrease as L/D ratio increases. These coefficients are of negative values and near about the same. Figure 12 depicts that C_{yy} increases as there is increase in L/D ratio and is found to be maximum at a ratio 2.4. It is also observed that for a particular L/D ratio C_{yy} is higher at lower value of characteristics length (l_m) and decreases as l_m decreases. Damped frequency of whirl (ω_d) is shown in Figure 13 and is found minimum at aspect ratio 1.6. It is also observed that for a particular L/D ratio damped frequency of whirl is higher at lower value of characteristics length (l_m) and decreases as l_m decreases. Damped frequency is higher at lower dam width ratio. Figure 14 represents the behavior of critical mass with characteristics length. Critical mass is higher at lower values of l_m, irrespective of dam width ratios and decreases as l_m increases. Critical mass is higher at higher value of dam width ratio for a particular L/D ratio. Figure 15 shows the threshold speed variation with l_m which shows that threshold speed ω_s increases up to a particular material length and then decreases with increase in l_m. Threshold speed is higher at higher dam width ratio for the same value of L/D ratio.

5. Conclusions

(i) By incorporating of pressure dam, relief track and modification of lubricant to micropolar fluid result in increase of load capacity with increase in the aspect ratios.

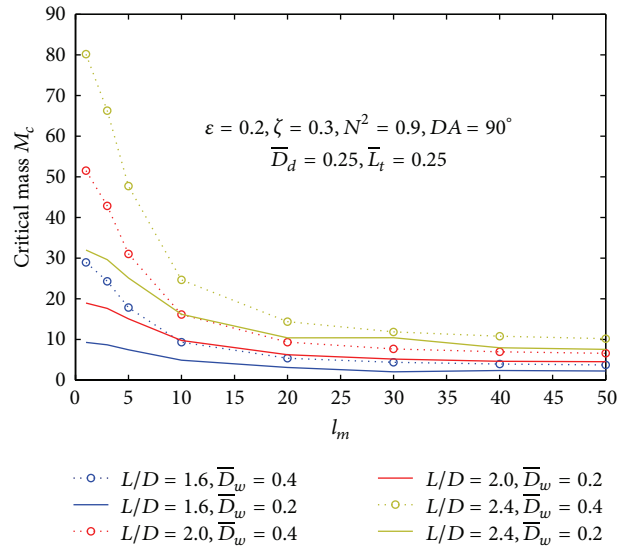

FIGURE 14: Variation of critical mass M_c as a function of characteristics length "l_m."

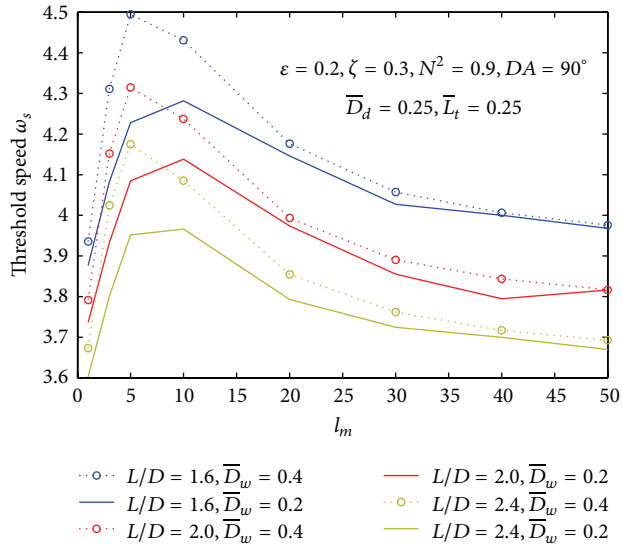

FIGURE 15: Variation of threshold speed ω_s as a function of characteristics length "l_m."

(ii) There is reduction in attitude angle for low value of characteristics length "l_m," but it increases with increase in characteristics length "l_m." Higher aspect ratios result in larger attitude angle. Lower attitude angle is observed at smaller dam width ratio.

(iii) Damped frequency of whirl is found to be lower at higher dam width ratio, while critical mass and threshold speed increase as dam width ratio increases.

(iv) Stability of two-lobe pressure dam increases by incorporating pressure dam with micropolar lubrication.

Appendix

Performance Characteristics

(1) Load Capacity. The load components are given by the expression

$$\overline{W}_v^{\,e} = \iint \overline{p}^e \cos\theta d\theta d\overline{z},$$
$$\overline{W}_h^{\,e} = \iint \overline{p}^e \sin\theta d\theta d\overline{z}. \tag{A.1}$$

To maintain the equilibrium of journal centre, horizontal components of load must be zero:

$$\overline{W}_h = 0. \tag{A.2}$$

(2) Fluid Film Stiffness Coefficients. Fluid film stiffness coefficients are calculated using the following expressions:

$$\overline{K}_{ij} = \frac{\partial \overline{W}_i}{\partial \overline{s}_j}, \quad (i = x, y), \tag{A.3}$$

where i is the direction of force.

$\overline{s}_j$ = direction of journal center displacement ($\overline{s}_j = \overline{x}_j, \overline{z}_j$).

(3) Fluid Film Damping Coefficients. Consider

$$\overline{C}_{ij} = \frac{\partial \overline{W}_i}{\partial \dot{\overline{s}}_j}, \quad (i = x, y), \tag{A.4}$$

where $\dot{\overline{s}}_j$ represents the velocity component of the journal center ($\dot{\overline{s}}_j = \dot{\overline{x}}_j, \dot{\overline{z}}_j$).

(4) Stability Parameters. When the natural frequency of journal system reaches the damped frequency of whirl, instability arises. The damped frequency of whirl ω_d is given below [11]:

$$\omega_d^{\,2} = \frac{(K_{xx} - \lambda)(K_{yy} - \lambda) - K_{xy}K_{yx}}{C_{xx}C_{yy} - C_{xy}C_{yx}}, \tag{A.5}$$

where

$$\lambda = \frac{K_{xx}C_{yy} + K_{yy}C_{xx} - K_{xy}C_{yx} - K_{yx}C_{xy}}{C_{xx} + C_{yy}}. \tag{A.6}$$

A negative value of ω_d means no whirl is there.

Critical mass M_c is numerically represented as $M_c = \lambda/\omega_d^{\,2}$.

Threshold speed $\omega_s = \sqrt{\overline{M}_c/W}$.

Nomenclature

c: Radial clearance (m)
c_m: Minor clearance (m)
D: Journal diameter (m)
D_w, L_t: Dam width, relief track width (m)
$\overline{D}_w$, $\overline{L}_t$: D_w/L, L_t/L
D_d: Dam depth (m)
$\overline{D}_d$: D_d/c
DA: Dam angle in degree (degree) (measured in anticlockwise from positive x-axis)
h: Film thickness (m)
$\overline{h}$: Nondimensional film thickness
L: Bearing axial length (m)
l_m: Nondimensional characteristics length
N^2: Coupling number
O_u, O_l: Upper lobe centre, lower centre
O_j, O_b: Journal centre, bearing centre
p: Fluid film pressure (N/m^2)
$\overline{p}$: Nondimensional film pressure
R: Radius of journal (m)
U: Velocity of journal (m/s)
$\overline{W}_h$, $\overline{W}_v$: Nondimensional load components
X, Y, Z: Cartesian coordinate axis.

Greek

ω: Angular speed of journal (rad/s)
ε: Eccentricity ratio
ε_1, ε_2: Lobe eccentricity ratio, e_1/c, e_2/c
ξ: Ellipticity ratio
δ_v: $\delta_v = d_v/c$
ϕ: Attitude angle of the bearing (radian)
ϕ_1, ϕ_2: Angles (radian)
μ: Viscosity of the Newtonian fluid (N-s/m^2).

Conflict of Interests

The authors declare that there is no conflict of interests regarding the publication of this paper.

References

[1] Y. Hori, "A theory of oil whip," *Journal of Applied Mechanics*, vol. 26, no. 2, pp. 189–198, 1959.

[2] R. H. Badgley and J. F. Booker, "Turborotor instability: effects of initial Transients on plane motion," *Journal of Lubrication Technology*, vol. 91, no. 4, pp. 625–630, 1969.

[3] S. B. Shenoy and R. Pai, "Steady state performance characteristics of a single pad externally adjustable fluid film bearing," *Journal of Advanced Mechanical Design, Systems, and Manufacturing*, vol. 2, no. 5, pp. 937–948, 2008.

[4] J. W. Lund and K. K. Thomson, "A calculation method and data for the dynamic coefficient of oil-lubricated journal bearings," in *Proceedings of the ASME Design and Engineering Conference*, pp. 1–28, New York, NY, USA, 1978.

[5] A. Kumar, R. Sinhasan, and D. V. Singh, "Performance characteristics of two-lobe hydrodynamic journal bearings," *Journal of Tribology*, vol. 102, no. 4, pp. 425–429, 1980.

[6] S. C. Soni, R. Sinhasan, and D. V. Singh, "Performance characteristics of noncircular bearings in laminar and turbulent flow regimes," *ASLE Transactions*, vol. 24, no. 1, pp. 29–41, 1981.

[7] A. Singh and B. K. Gupta, "Static and dynamic properties of oil films in displaced centres elliptical bearings," *Proceedings of the Institution of Mechanical Engineers, Part C: Journal of Mechanical Engineering Science*, vol. 197, no. 3, pp. 159–165, 1983.

[8] J. C. Nicholas, L. E. Barrett, and M. E. Leader, "Experimental Theoretical comparison of instability onset speeds for a three mass rotor supported by step journal bearings," *Journal of Mechanical Design, Transactions of the ASME*, vol. 102, no. 2, pp. 344–351, 1980.

[9] J. C. Nicholas and P. E. Allaire, "Analysis of step journal bearings—finite length stability," *ASLE Transactions*, vol. 23, no. 2, pp. 197–207, 1980.

[10] N. P. Mehta, A. Singh, and B. K. Gupta, "Stability of finite elliptical pressure dam bearings with rotor flexibility effects," *ASLE Transactions*, vol. 29, no. 4, pp. 548–557, 1986.

[11] K. Prabhakaran Nair, V. P. Sukumaran Nair, and N. H. Jayadas, "Static and dynamic analysis of elastohydrodynamic elliptical journal bearing with micropolar lubricant," *Tribology International*, vol. 40, no. 2, pp. 297–305, 2007.

[12] N. P. Mehta and S. S. Rattan, "Performance of three-lobe pressure-dam bearings," *Tribology International*, vol. 26, no. 6, pp. 435–442, 1993.

[13] N. P. Mehta and S. S. Rattan, "Stability analysis of three-lobe bearings with pressure dams," *Wear*, vol. 167, no. 2, pp. 181–185, 1993.

[14] A. Eringen, "Theory of micropolar fluids," *Journal of Mathematics and Mechanics*, vol. 16, pp. 1–18, 1966.

[15] A. E. Yousif and T. M. Ibrahim, "Lubrication of a slider bearing with oils containing additives and contaminants," *Wear*, vol. 81, no. 1, pp. 33–45, 1982.

[16] H. Hayakawa, "Slow viscous flows in micropolar fluids," *Physical Review E*, vol. 61, no. 5, pp. 5477–5492, 2000.

[17] M. Balaram, "Micropolar squeeze films," *Journal of Lubrication Technology*, vol. 97, no. 4, pp. 635–637, 1975.

[18] S. Das, S. K. Guha, and A. K. Chattopadhyay, "Linear stability analysis of hydrodynamic journal bearings under micropolar lubrication," *Tribology International*, vol. 38, no. 5, pp. 500–507, 2005.

[19] A. D. Rahmatabadi, M. Nekoeimehr, and R. Rashidi, "Micropolar lubricant effects on the performance of noncircular lobed bearings," *Tribology International*, vol. 43, no. 1-2, pp. 404–413, 2010.

[20] A. D. Rahmatabadi, M. Sefid, R. Rashidi Meybodi, and M. Nekoeimehr, "Effects of bearing orientation on the static performance of micropolar lubricated lobe bearings," *Proceedings of the Institution of Mechanical Engineers, Part J: Journal of Engineering Tribology*, vol. 226, no. 1, pp. 3–13, 2012.

[21] S. Sharma and S. S. Rattan, "Micropolar lubricant effects on the performance of a two- lobe bearing with pressure dam," *International Journal of Engineering Science & Technology*, vol. 2, no. 10, pp. 5637–5646, 2010.